Isa thesis v2.

very short, expert-level.
Suggestions for ways to make more educational:
- show N(partons) or N(genjets) for monojet signal or Z(νν)+jets (or both)
- show ChF and/or N(particles) @ gen level for some dijet selection in your 2016 dataset vs MC. (unless this comes in LHC chapter)
- show N(pileup)
- make a sketch of what an event looks like.

4 Event Simulation and Reconstruction

In order to use the recorded data, the obtained signals coming from various parts of the detector must be reconstructed to be able to identify the particles in the event. Additionally, to compare the experimental results with theory, events are generated and the resulting signals in the detector are simulated, as detailed in Sections 4.1 and 4.2, respectively. The event reconstruction is detailed in Section 4.3. Finally, some details about the simulation of strongly interacting massive particles (SIMPs) are given in Section 4.4.

4.1 Event generation

at

The event structure at the LHC is complicated by the composite nature of protons, as well as the attainable high momentum transfers. A number of aspects must therefore be taken into account when generating events, such as parton distribution functions (PDFs), hard scattering, the parton shower, hadronization, and additional activity in the event.

I don't get how that makes things complex

Two partons, meaning the quark or gluon constituents of the colliding protons, will interact with a certain probability for a given momentum transfer. This is parametrized by the PDFs $f(x, Q^2)$, were x is the proton's momentum fraction of the partons and Q^2 is the momentum transfer scale. Experimentally determined PDFs are available from various groups, including e.g. CTEQ [6], MRST/MSTW [7], and NNPDF [8]. An example of such PDFs obtained by the NNPDF group is shown in Figure 4.1. The PDFs are ~~then~~ ~~used~~ to calculate the matrix element of the hard scattering, which is the process of interest where the two colliding partons create high-energetic final state particles. This is done using an event generator, such as MADGRAPH5_aMC@NLO [9] and POWHEG [10]. With MADGRAPH5_aMC@NLO the matrix element can be calculated analytically at tree-level or leading order (LO), and since the addition of aMC@NLO at next-to-leading order (NLO) as well. This generator was used to generate most of the background processes for the Monojet analysis detailed in Chapter 5 and for the SIMP signal used in Chapter 6. POWHEG is able to generate events using NLO computations, but only for a relatively limited number of physics processes. In this thesis, background processes from single-top production were generated with this program. Since NLO calculations are more time-consuming, one can also scale a LO cross section to the NLO level by using a so-called k-factor, defined as the ratio of the NLO and LO cross sections. However, these k-factors often need to be determined as a function of the relevant kinematic variables as they depend on the kinematic phase space and the probed energy scale.

ME calc. is independent, PDFs are convoluted with ME

not sure this is the right word...

sounds as if it's equivalent

Since the colliding partons have a color charge, the hard scattering will be accompanied by a cascade of radiation from QCD processes. This radiation can originate from the incoming partons, which is referred to as initial state radiation (ISR), or the outgoing partons in the final state, the so-called final state radiation (FSR). The perturbative evolution of the cascade can be modeled using the DGLAP (Dokshitzer-Gribov-Lipatov-Altarelli-Parisi) equations [11–13]. These equations describe the time evolution of the

defined?

these should be easy plots to make 1 time ~ manually
SaveAs(.C) also for cosmetic changes later

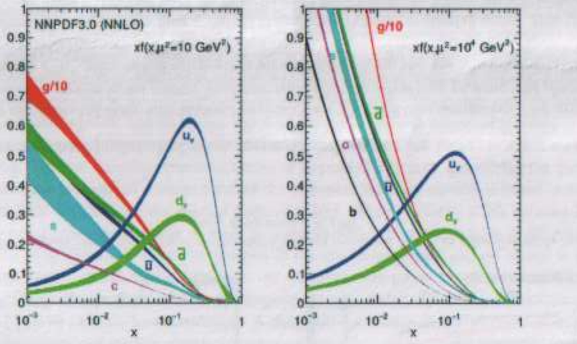

Figure 4.1: The parton distribution functions times the momentum fraction x at energy scales 10 GeV² (left) and 10 000 GeV² (right), obtained in NNLO NNPDF3.0 global analysis [8].

probability of a 'mother' parton to split into 'daughter' partons at an energy scale Q^2. The momentum of the mother is then divided among the daughter partons, which can in turn split into other partons at a lower Q^2 scale. The cascade continues down to an energy scale Λ_{QCD} where the strong coupling constant becomes unity.

here you could add that higher p_T's lead to more radiated partons at certain p_T, which is relevant for the SIMPs

The next step after the showering is the hadronization of the colored particles produced in the parton shower, transforming them into color-neutral hadrons. Since this happens at low energy scales where the perturbative approach of QCD is not valid, phenomenological models have to be used. For most of the processes considered in this thesis, the showering and hadronization is done with PYTHIA 8 [14], using a standard set of parameters which were tuned to reproduce the experimental data.

In addition to ISR and FSR, also beam remnants and multiple parton interactions give rise to additional activity in the event, referred to as the underlying event. After the partons participating in the hard scattering are extracted, the remainder of the protons have a non-zero color charge. The creation of additional hadrons during the hadronization is therefore possible. Multiple parton interactions represent additional interactions which can take place between other incoming partons. Finally, additional collisions between other protons in the same bunch crossing or from a previous bunch crossing, respectively referred to as in-time and out-of-time pileup, add extra activity in the event.

* could go in first plot earlier
* potentially show ISR & FSR jet separately (though that's a little harder)

4.2 Detector simulation

After being generated, the collision events are passed on to the CMS detector simulation, which is based on the GEANT 4 [15] simulation toolkit. This toolkit provides a description of the interaction between particles and the detector material, including effects such as bremsstrahlung of charged particles, photon conversions, energy loss of charged particles by ionization, and the showering of electrons, photons and hadrons in the calorimeters due to interaction with the material. The CMS simulation package contains the geometry of the detector with all the sensitive layers designed to detect the traversing particles, as well as the dead material regions consisting of e.g. support structures, cables and cooling pipes. A precise map of the magnetic field is also included in order to simulate the curvature of the charged particles correctly.

Next, the electronic response produced by the hits in the active detector material is simulated, resulting in an event content similar to the output of the real detector. At this point the effect of pileup is also included by adding detector hits of generated proton-proton interactions on top of the hits resulting from the main interaction. Most of the simulated event samples used in this thesis are processed using this detector simulation. However, the interaction of new particles that can arise from specific theory models is not always readily described in GEANT. This is the case for the signal samples used in the analysis

also: digitization, data transmission, any reconstruction in electronics such as zero-suppression or cluster reco, etc.

described in Chapter 6, so an additional step was needed in order to simulate strongly interacting massive particles (SIMPs) in the CMS detector. — described in Section 6.6.

4.3 Event reconstruction

Once the detector response has been simulated, the obtained events can be reconstructed. The same method is applied for these simulated events and for data coming from the detector. First, the reconstruction of tracks is performed, with a specific track reconstruction for electrons and muons. Furthermore, the calorimeter deposits, generated by electrons, photons, and hadrons, are grouped into clusters. Additionally, the reconstruction is further improved by using the so-called particle flow (PF) algorithm. This algorithm greatly improves the performance for jet and hadronic τ decay reconstruction, missing transverse energy momentum determination, as well as electron and muon identification. Finally, the obtained particle flow (PF) candidates are clustered into jets, and the missing transverse energy can be derived.

read before
see these comments

4.3.1 Track and vertex reconstruction

The tracks of charged particles going through the CMS tracker are reconstructed with an iterative tracking approach. This is used to cope with the high occupancy and consequently high combinatorics. Additionally, the first iterations search for tracks with less possible combinations, such as tracks with many pixel hits or a high momentum. After every iteration, the hits associated with the found track are removed to reduce the combinatorics. Each iteration consists of four steps:

1. **Seed generation.** In this first step hits are combined into seeds for the subsequent track finding. In the initial iterations pixel triplets are used, then pixel pairs, in order to take gaps or non-working modules into account. Next, mixed pixel/strip triplets are taken, and finally strip-only seeds are used. These additional iterations improve the acceptance in p_T and in displacement with respect to the primary vertex.

2. **Track finding.** The seeds are used as starting point for a Kalman filter algorithm. This method extrapolates the seed trajectory outward to the next layer, taking into account potential energy loss and multiple scattering. If compatible hits are found in the next layer, the parameters of the trajectory are updated. This process continues until the outermost layer of the tracking system. Using this method, a given seed can generate multiple tracks, or different tracks can share hits. A trajectory cleaner therefore determines the fraction of hits the tracks have in common and discards the track with the lowest number of hits when there are too many shared hits. If both tracks have the same number of hits, the track with the largest χ^2 value is removed.

3. **Track fitting.** The track parameters are then refitted using a Kalman filter and smoother, taking all hits determined in the track finding step into account.

4. **Track selection.** Finally, the tracks are selected based on quality requirements, such as the number of layers that have hits, the χ^2/dof, and the distance to a primary vertex. This greatly reduces the fraction of reconstructed tracks that are fake.

The performance of the track reconstruction is excellent, and a high track-finding efficiency is obtained [16] while keeping the rate of fake tracks negligible. The highest tracking efficiency is obtained for muons, which traverse the full detector volume and have an improved momentum resolution due to tracking information from the muon detectors giving a long lever arm. For isolated muons with p_T between 1 and 100 GeV the tracking efficiency is higher than 99% for the entire η coverage of the tracker, as can be seen from the left plot in Figure 4.2. The p_T resolution is about 2-3% for a muon with p_T = 100 GeV up to $|\eta| < 1.6$, but worsens for higher pseudorapidities. Different types of particles interact differently with the detector material. Charged hadrons, for example, are also subject to elastic and inelastic nuclear interactions and have a tracking efficiency of 80-95% depending on pseudorapidity and transverse momentum, as shown in the right plot of Figure 4.2.

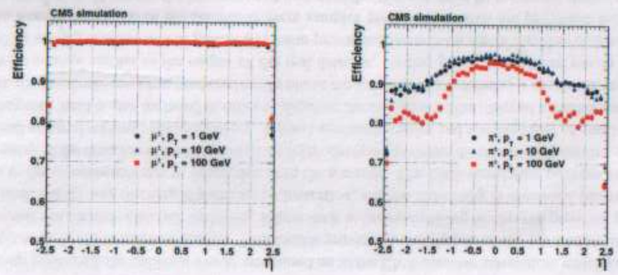

Figure 4.2: The muon efficiency (left) and pion efficiency (right) as a function of pseudorapidity, for multiple transverse momenta. [16]

Finally, the primary vertex is reconstructed from the tracks. Since the collisions happen between bunches of protons, multiple protons will be colliding at the same time. The extra collisions, next to the potentially interesting collision, are referred to as pile-up interactions. The particles generated in these collisions are all detected simultaneously and form a challenge to disentangle them from the particles coming from the to be studied interaction.

The reconstruction is done in 2 steps: first the tracks that appear to originate from the same interaction vertex are clustered, then a fitting procedure computes the vertex parameters and assigns a weight to each associated track, reflecting the probability that it corresponds to the considered vertex. Figure 4.3 shows the reconstruction efficiency and the resolution of the primary vertex. The more tracks, the better the vertex is constrained and thus the better the resolution.

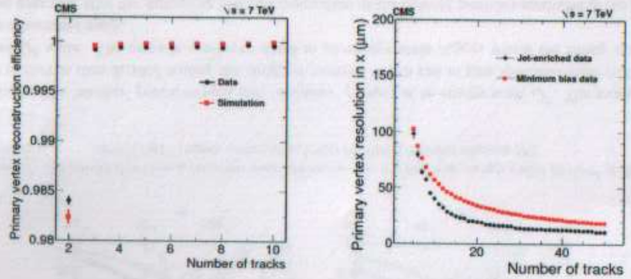

Figure 4.3: The primary vertex reconstruction efficiency (left) and resolution (right) as a function of the number of tracks associated to it. [16]

4.3.2 Electron and isolated photon reconstruction

Electrons are reconstructed using information from both the tracker and the calorimeters. Due to the large amount of material present in the tracker, electrons will emit bremsstrahlung photons, and photons will often convert into e^+e^- pairs, which can again radiate bremsstrahlung photons. ~~The electron and photon reconstruction is therefore very similar.~~ — only a piece of it.

For electrons, a Gaussian-sum filter (GSF) [17] candidate is taken as starting point. This GSF candidate is obtained using 2 different methods to reconstruct the electron track from the hits in the tracker, which should gather all radiated energy from the electron. First, the ECAL-based approach is used,

~~and this is input to GSF tracker and full electron reco (it needs now ... if the algo is done collecting hits)~~

grouping ECAL clusters into superclusters. These superclusters collect the energy of the electron and the bremsstrahlung photons in a small η window and a large ϕ window, taking the bending of the electron track in the magnetic field into account. The supercluster energy and position is then used to estimate the position of the corresponding hits in the tracker layers. Subsequently, the tracker-based approach is used to ~~reconstruct~~ electrons missed by the ECAL-based method. In this case, all the tracks from the iterative tracking with transverse momentum larger than 2 GeV are used. Next, the specific electron tracking is performed, using a GSF fit, which is more adapted to electrons than the Kalman filter used in the iterative tracking, as it describes the energy loss in each tracker layer. The electron seeds obtained with both methods are merged and used as input for the full electron tracking, which is performed with twelve GSF components. The obtained electron tracks are then linked to ECAL clusters by the PF algorithm, as described in Section 4.3.4. In the case of isolated photons, a candidate is seeded from an ECAL supercluster with transverse energy larger than 10 GeV which is not linked to a GSF track.

find

on all these candidates (?)

maybe switch order of this and next sentence

too much detail; cannot be understood.

separate section describe ID and 2 vetoes we use.

The total energy of the accumulated ECAL clusters is corrected for the energy that was lost in the process of reconstruction, using analytical functions of the energy and pseudorapidity. The applied corrections can be as large as 25%, at low transverse momentum and at $|\eta| = 1.5$, where the material density in the tracker is largest. The energy of the electron is then obtained from a combination of the corrected energy and the momentum of the GSF track, while the direction of the electron is taken from the GSF track. For photons, the corrected energy and the direction of the supercluster are used.

Additionally, the electron and photon candidates must satisfy identification criteria to be retained. In the case of electrons a boosted decision tree is used, combining fourteen variables including the amount of energy radiated and the ratio between the energies gathered in HCAL and ECAL, while for photons the candidates must be isolated from other tracks and calorimeter clusters, and the energy distribution in the ECAL and the ratio between the HCAL and ECAL energies must be compatible with the expectation from a photon shower.

defined?

4.3.3 Muon reconstruction

defined?

Muon tracking is performed using 2 complementary approaches. The first method starts from standalone muons which are reconstructed from hits in the muon detectors using pattern recognition. The standalone muons are then matched to tracks in the tracker, and the hits are combined to form a global muon track. This global muon fit improves the momentum resolution compared to the tracker-only fit at muon momenta larger than 200 GeV.

defined?

For momenta below 10 GeV, muons often fail the global muon conditions which require the muon to penetrate through more than one muon detector plane, due to the large multiple scattering in the return yoke. In this case, tracker ~~muon reconstruction~~ is more efficient since it only requires one muon segment. Each track in the tracker with a transverse momentum larger than 0.5 GeV and a total momentum larger than 2.5 GeV is therefore extrapolated to the muon system and if at least one matching track segment is found, it is retained as muon candidate.

Within the geometrical acceptance of the muon system about 99% of the muons are reconstructed, either as global muon or as tracker muon and frequently as both. Global and tracker muons that share the same track inside the tracker are merged into a single candidate. Muons that are only reconstructed as standalone muons have a worse momentum resolution compared to the global and tracker muons.

but those are not part of the list, right?

Charged hadrons can be misreconstructed as muons if e.g. a part of the hadron shower reaches the muon system. In order to improve the muon identification, the PF muon identification algorithm described in Section 4.3.4 also matches energy deposits in the ECAL and HCAL with the muon track.

4.3.4 Particle flow

The particle flow (PF) algorithm reconstructs so-called particle flow candidates by combining information from all different CMS subdetectors, linking different elements, such as tracks in the tracker, calorimeter clusters, and muon tracks. The obtained collection of particle candidates is subsequently used to reconstruct jets and to determine the missing transverse energy.

add that this gives a global event picture where each particle is uniquely identified

in particular

for all tracks

In a first step, the PF algorithm identifies charged particle tracks, as defined in Section 4.3.1, and Sections 4.3.2 and 4.3.3 for electron and muon tracks, ~~respectively~~. At the same time, the calorimeter clusters are reconstructed with a clustering algorithm designed specifically for the PF event reconstruction. In this algorithm, cluster seeds are first identified as local energy maxima with respect to the four or eight closest cells, if the energy deposited in the cell is above a given seed threshold. The clusters are then formed by accumulating neighboring cells with an energy above a given cell threshold, suppressing noise.

The PF elements in the different subdetectors are then connected by a link algorithm which avoids any double counting. The link algorithm produces blocks of associated elements, quantifying the quality of the link by defining a geometrical distance between the elements. When an element is linked to multiple other elements, only the link with the shortest distance is kept. More precisely, a link between a track in the tracker and a calorimeter cluster is made by extrapolating it from the last hit in the tracker to the calorimeters. The distance between the position of the extrapolated track and the cluster in the (η, ϕ) plane is then used to define the link distance. At the interaction points between the track and the tracker layers, tangents to the GSF tracks are extrapolated to the ECAL in order to collect the energy of photons radiated by electron bremsstrahlung. A dedicated conversion finder was also developed to identify bremsstrahlung and prompt photon conversions into e^+e^- pairs. Links between calorimeter clusters are established outside of the tracker acceptance, or between the preshower and ECAL clusters in the preshower acceptance. In this case the link distance is also defined as the distance between the position of the clusters. Charged particle tracks can also be linked by a common secondary vertex. Finally, the PF muon identification algorithm associates the muon tracks to the muon energy deposits in the ECAL and HCAL, to improve the muon identification performance.

~~In a next step, the~~ PF blocks are classified as muons, electrons, or isolated photons. The corresponding elements are then excluded from further consideration. Once electrons, muons, and isolated photons have been identified, the remaining elements are identified as charged hadrons, neutral hadrons, or photons (produced in jets). Within the tracker acceptance, the ECAL clusters not linked to any track are classified as photons, while the clusters in the HCAL without a matched track are labeled as neutral hadrons. Outside of the tracker acceptance, charged and neutral hadrons can not be distinguished. ECAL clusters linked to an HCAL cluster are then assumed to arise from the same hadron shower, and the estimated energy for these particles is the sum of the energy deposited in the ECAL and the HCAL. The remaining clusters are then linked to one or several tracks in order to reconstruct the charged hadrons.

drop?

but you're still outside of tracker acceptance!

4.3.5 Jet reconstruction

or jet particles

Jets are reconstructed with the anti-k_T algorithm [18], which clusters either the particles reconstructed by the PF algorithm (PF jets) or the energy deposits in the calorimeters (Calo jets). This procedure takes into account the transverse momentum p_T, also called k_T, of the particles and the distance between particles, defined as

$$\Delta R_{ij} = \sqrt{(\eta_i - \eta_j)^2 + (\phi_i - \phi_j)^2}. \tag{4.1}$$

The strategy consists of the following steps:

1. For every pair of particles i and j, a distance d_{ij} defined as

$$d_{ij} = \min\left(\frac{1}{p_{Ti}^2}, \frac{1}{p_{Tj}^2}\right) \frac{\Delta R_{ij}^2}{R^2} \tag{4.2}$$

is calculated.

2. For every particle i, a distance d_{iB} to the beam pipe is calculated with

$$d_{iB} = 1/p_{Ti}^2. \tag{4.3}$$

3. The minimum of d_{ij} and d_{iB} is then determined.
4. If it is d_{ij}, particles i and j are recombined into a new particle by adding the four-momenta of the particles. If it is d_{iB}, particle i is declared to be a jet and it is removed from the list of particles.

5. This is repeated until no particles remain.

In this clustering algorithm, the parameter R determines what is called a jet. If a particle i has no other particles within a distance R, d_{iB} will be smaller than d_{ij} and the particle will become a jet. A consequence of this is that an arbitrarily soft particle can become a jet, and therefore a minimum transverse momentum for a jet to be of interest is defined.

The anti-k_T algorithm favors clustering around hard particles, and the jets then grow outward from this seed. However, since it still involves a combination of energy and angle in the distance measure, this is a collinear-safe growth, meaning that the jet will not change when one of the particles of the jet is split collinearly. This algorithm is also infrared-safe, i.e. the same set of jets is obtained when soft particles are emitted. and gives rise to circular jets. — separate sentence earlier in paragraph (for intuition) also: R ~ cone size

A reliable determination of the jet energy is not straightforward, since many effects can distort the energy estimation, such as the calorimeter response, the limited particle reconstruction efficiency, the underlying event, the pileup, and the charged particles bending out of the jet cone due to the strong magnetic field. The pileup is mitigated by applying charged hadron subtraction (CHS), which consists of removing charged hadrons associated with vertices other than the primary vertex from the list of PF candidates. Additionally, the jet energy is corrected using a factorized approach, as illustrated in Figure 4.4, with the following steps:

this goes fast. Also use "we"

- **Pileup correction (L1).** The first level of jet energy corrections is applied event-by-event and jet-by-jet, and is determined from simulation. It is dependent on the pseudorapidity and transverse momentum of the jet, the average p_T density in the event, and the effective jet area. This effective area is determined by injecting a large number of very soft particles in the event before the jet clustering. The spread of the soft particles in each jet then defines the jet area.
- **Relative η and absolute p_T corrections (L2L3).** This correction is also obtained from simulations and corrects for the non-uniform response of the calorimeters in η and p_T.
- **Residual η and p_T corrections (L2L3Residual).** Since the L2L3 correction is derived from simulation, additional residual corrections are needed in order to correct for the remaining small differences between the jet response in data and simulation. These corrections are typically of the order of a few percent.

you could add this is the bulk of the energy correction, potentially say a little bit more

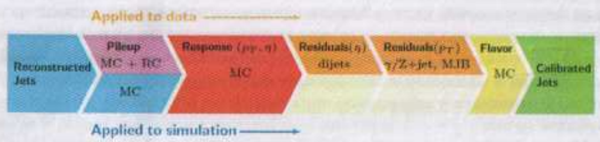

Figure 4.4: Graphical overview of the factorized approach used at CMS to apply jet energy corrections.

you could say "from [...]", but you may remark to simplify because several things in here are not explained

optionally

Finally, a set of identification criteria are applied on the PF jets. A jet is required to consist of at least two particles. For jets in the region $|\eta| < 2.7$, the fraction of energy coming from either neutral hadrons or photons should not exceed 99%. Additionally, for jets restricted to the tracker acceptance ($|\eta| < 2.4$), there should at least be some energy deposited in the HCAL, the jet should contain 1 or more charged constituent, and the fraction of energy corresponding to electrons or photons should not exceed 99%.

need something on b-tagging and tau reco, since we have many other words can be short

4.3.6 Missing transverse ~~energy~~ momentum reconstruction

While most particles produced in the collisions can be reconstructed from the hits and energy deposits in the detector, some collision products might not leave energy deposits in tracker, calorimeters or muon system. This makes an accurate reconstruction of this type of particles rather challenging. Another method is therefore used, based on indirect observations. As the detector is hermetically closed such that all other particles in the event can be detected, the missing transverse ~~energy~~ momentum can be determined. This

impossible? what was the 1st method? maybe use "alternatively"

momentum ignore

~~energy then corresponds to all undet~~ected particles in the event, and can be calculated from the vectorial sum of the transverse momenta of all the observed final state particles:

$$\vec{E}_T^{miss} = -\sum \vec{p}_T. \quad (4.4)$$

You may define $E_T^{miss} = |\vec{E}_T^{miss}|$ the norm

where the sum runs over all reconstructed PF particles.

A notable example of particles leaving no hits or energy deposits behind are neutrinos, as they are neutral and weakly interacting and will therefore traverse the entire detector. Other hypothetical neutral weakly interacting particles, which are being searched for in many physics analyses, would escape the detector without producing hits as well.

maybe be more specific, relate to unhindered

4.4 Simulation of the SIMP signal

For the generation of the SIMP signal, the model Lagrangian given in equation ?? is implemented in FEYNRULES 2.0 [19]. Next, the matrix element is calculated at LO and events are generated using MADGRAPH 5. The subsequent parton shower and hadronization is done with PYTHIA 8, using tune CUEP8M1. Next, the events are simulated in the CMS detector using GEANT. However, the SIMPs are not included in the simulation, as their interaction with matter is not implemented in GEANT. The SIMPs were instead incorporated by adding an additional step to the standard reconstruction described in Section 4.3. In this additional step the SIMPs are directly converted to neutral PF candidates and merged with the rest of the PF candidates. The standard pileup corrections, jet clustering, and charged hadron subtraction are then applied in order to obtain the resulting jets, denoted here as P2PF jets.

Is this repeated somewhere? otherwise I'd expect a section for DM as well. It would fit.

In order to validate this method, a second sample was produced using neutrons instead of SIMPs and applying the same additional step. In this case the the neutrons will also be correctly reconstructed by the standard reconstruction. The reconstructed PF candidates that are matched to the generated neutrons were therefore removed before injecting the converted generated neutrons to the collection of PF candidates. This sample is then used to evaluate the difference with a standard neutron sample where the full GEANT simulation is done. Neutrons were chosen because of their resemblance to the SIMPs as single neutral particles generating a hadronic shower.

explain why neutrons

ah ok. maybe move earlier

The two leading generator-level jets (GEN) can then be compared to the uncorrected P2PF jets from the custom sample and the PF jets from the standard sample. The transverse momentum of these jets is compared in Figure 4.5. This shows that the jet energy resolution (JER) is not described properly, since the additional step directly converts generated particles to PF candidates without taking into account any other effects. In order to produce a more realistic simulation, the new PF candidates are therefore smeared with JER distributions derived using the uncorrected PF jets matching the neutrons in the standard neutron sample in bins of η and p_T. An example of this resolution is shown in Figure 4.6 for central neutrons with low and high transverse momentum.

After applying this smearing, the P2PF jets are processed with the standard sequence of charged hadron subtraction, jet clustering, L1FastJet, and L2/L3 corrections. The comparison of the corrected P2PF jets and the standard corrected PF jets is shown in Figure 4.7 for the neutron sample, validating that the jet transverse momentum is now correctly smeared. The JER distributions are also compared in Figure 4.8 and fitted with a Crystal Ball function, showing compatible parameters. This demonstrates that the procedure, where the JER distributions derived from a neutron sample are used to smear the PF candidates from generator-level SIMPs, can sufficiently accurately simulate SIMPs in a realistic detector. assuming SIMPs are neutronlike.

This is rather heavy to read. You can use more space to be more educational.
One simplification you could do is skip the story of Figure 4.5. Historically we went through that, but in hindsight it is obvious we need to smear the genlevel neutrons/SIMPs.

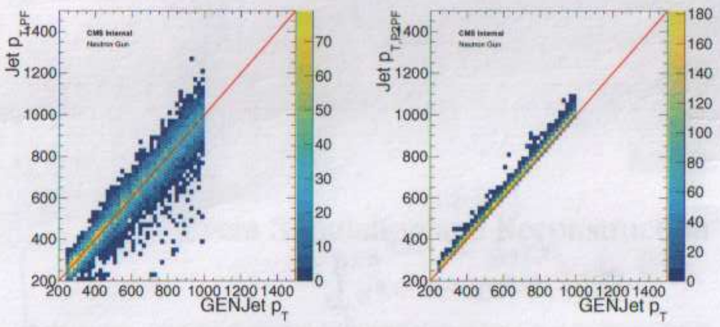

Figure 4.5: Comparison of the transverse momentum of the generator-level jets to the PF jets (left) and P2PF jets (right) without jet energy resolution smearing, using a neutron sample.

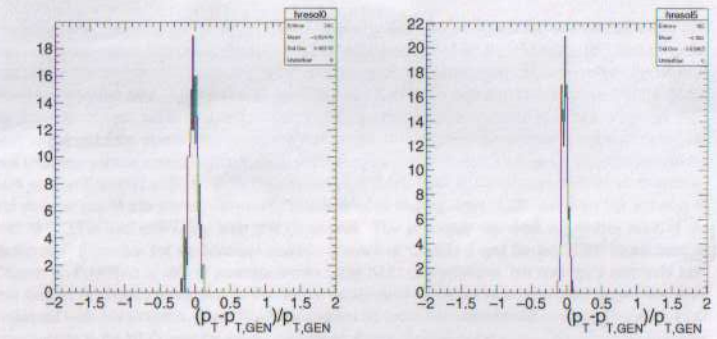

Figure 4.6: The jet energy resolution of neutrons with $0 < |\eta| < 0.5$ and $200\,\mathrm{GeV} < p_T < 300\,\mathrm{GeV}$ (left) or $700\,\mathrm{GeV} < p_T < 800\,\mathrm{GeV}$ (right).

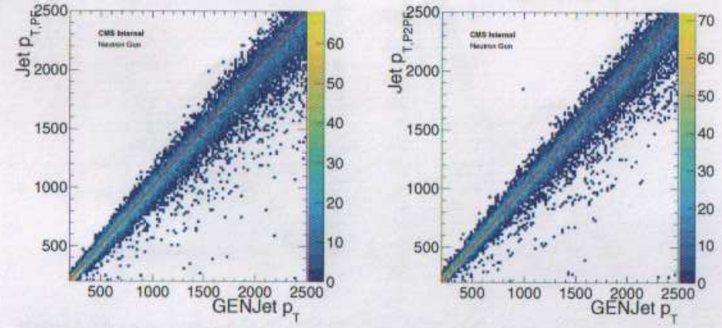

Figure 4.7: Comparison of the transverse momentum of the generator-level jets to the PF jets (left) and P2PF jets (right) in the region $0 < |\eta| < 0.5$ with jet energy resolution smearing, using a neutron sample.

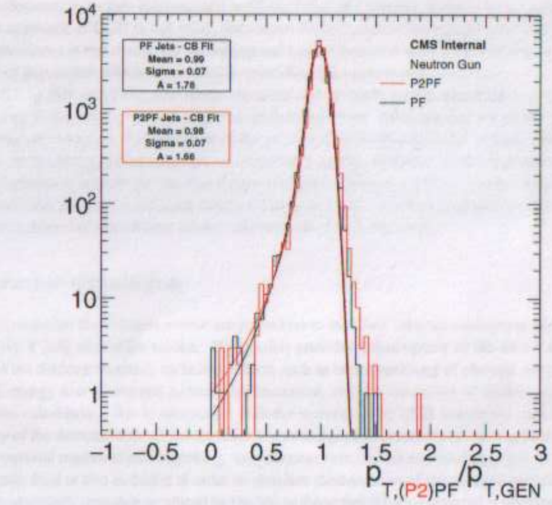

Figure 4.8: The jet energy resolution of the corrected P2PF jets (red) and PF jets (black), fitted with a Crystal Ball function.